International Journal of Heat and Mass Transfer 126 (2018) 1111–1119

Contents lists available at ScienceDirect

International Journal of Heat and Mass Transfer

journal homepage: www.elsevier.com/locate/ijhmt

Numerical solution of multi-dimensional transient nonlinear heat conduction problems with heat sources by an extended element differential method

Miao Cui [a,b], Bing-Bing Xu [a], Jun Lv [a], Xiao-Wei Gao [a,*], Yuwen Zhang [b,*]

[a] State Key Laboratory of Structural Analysis for Industrial Equipment, Dalian University of Technology, Dalian 116024, PR China
[b] Department of Mechanical and Aerospace Engineering, University of Missouri, Columbia, MO 65211, USA

ARTICLE INFO

Article history:
Received 7 April 2018
Received in revised form 16 May 2018
Accepted 19 May 2018
Available online 29 May 2018

Keywords:
Heat conduction
Transient state
Temperature-dependent thermophysical properties
Element differential method

ABSTRACT

In this paper, the element differential method is extended to solve a transient nonlinear heat conduction problem with a heat source and temperature-dependent thermophysical properties for the first time. The transient term is discretized by employing a finite difference scheme. An iterative methodology is developed to deal with the nonlinearity caused by temperature-dependent thermophysical properties. Examples of two-dimensional (2D) and three-dimensional (3D) problems are given to validate the present method for solving multi-dimensional transient nonlinear heat conduction problems. The results show that the present EDM provides a promising way that is effective and with high accuracy for solving multi-dimensional transient nonlinear heat conduction problems.

1. Introduction

Solving multi-dimensional transient nonlinear heat conduction problems is of extreme importance in many engineering applications [1–5], in which multi-dimensionality, transient term and temperature-dependent thermophysical properties are all involved. For solutions of heat conduction problems, there are mainly three ways: analytical, numerical, and experimental. The analytical solutions are limited to very simple problems, while experiments are always expensive or difficult to be carried out. Therefore, numerical approaches are dominant, and various techniques have been proposed, such as the finite difference method (FDM) [6,7], finite volume method (FVM) [8,9], finite element method (FEM) [10,11], meshless method (MLM) [12,13], boundary element method (BEM) [14–16] and some other innovative techniques [17–19].

Each method has its advantage and disadvantage, which has been reviewed in detail in Ref. [20]. As for transient nonlinear heat conduction problems, FDM is more suitable to solve problem with simple geometric configurations, considering accuracy, stability and efficiency. FEM is most powerful for solving complicated problems with complex geometries, and several commercial software is available, such as ANSYS, ABAQUS, NASTRAN and so on. However, the FEM in the commercial software is difficult to be applied in inverse analysis [21–23] by using the complex variable differentiation method for determining sensitivity coefficients. BEM would require further treatment of residual domain integrals caused by the transient term and the nonlinearity.

Although heat conduction problems have been extensively investigated, few references, associated with new techniques, have simultaneously dealt with heat source, multi-dimensionality, transient term, and temperature-dependent thermophysical properties. This paper presents a general approach and attempts to solve multi-dimensional transient nonlinear heat conduction problems with heat sources.

Recently, Gao and coworkers have proposed a new approach [20,24,25], element differential method (EDM), for solving second-order differential equations. This approach is based on the use of isoparametric elements as used in the standard FEM. A set of explicit formulations to compute the first and second order spatial derivatives were derived for two-dimensional and three-dimensional problems. No any mathematical principles or integrations are required. EDM is a strong-form technique, and the most important feature of the proposed method is that the derived spatial derivatives can be directly substituted into the governing equation and boundary conditions to form the final system of algebraic equations. Therefore, the EDM is very easy to code and program in dealing with engineering problems with complicated governing

* Corresponding authors.
E-mail addresses: xwgao@dlut.edu.cn (X.-W. Gao), zhangyu@missouri.edu (Y. Zhang).

https://doi.org/10.1016/j.ijheatmasstransfer.2018.05.100
0017-9310/

Nomenclature

A	coefficients matrix
b	vector
c	mass specific heat, J/(kg °C)
h	heat convective coefficient, W/(m^2 °C)
J	Jacobian matrix
L	1D shape function
i, j, k, l, n	subscripts
m	the number of interpolation points
N	order of equations
N_α	shape function
Q	heat source, W/m^3
q	heat flux, W/m^2
R	residual
T	temperature, °C
t	time, s
w	relaxation factor
$\boldsymbol{x}$	vector of unknowns
x_i	*the* i^{th} coordinate, m
x	x coordinate, m
y	y coordinate, m
z	z coordinate, m

Greek symbols

Γ	the boundary
Δ	change of variable
δ	Kronecker delta symbol
ρ	density, kg/m^3
ζ	intrinsic coordinate, m
η	intrinsic coordinate, m
λ	thermal conductivity, W/(m °C)
ξ	intrinsic coordinate, m

Subscripts

∞	surrounding

Superscripts

0	previous
k	*k*th iteration
m	*m*th

equations and boundary conditions, and the potential of the EDM in engineering applications has been partly validated in Ref. [20].

In the previous work, only the steady-state was considered. In this paper, the element differential method is extended to solve multi-dimensional transient nonlinear heat conduction problems with heat sources for the first time.

2. Transient nonlinear heat conduction problem

The governing equation of the transient nonlinear heat conduction problem with temperature-dependent thermophysical properties and a heat source can be expressed as

$$\frac{\partial}{\partial x_i}\left(\lambda_{ij}[T(x,t)]\frac{\partial T(x,t)}{\partial x_j}\right)+Q(x)=\rho[T(x.t)]c[T(x.t)]\frac{\partial T(x,t)}{\partial t}(x \in \Omega) \tag{1}$$

The boundary conditions are

$$T(x,t)=\overline{T} \qquad x\in\Gamma_1 \tag{2}$$

$$q(x,t)=-\lambda_{ij}[T(x,t)]\frac{\partial T(x,t)}{\partial x_j}n_i=\bar{q} \qquad x\in\Gamma_2 \tag{3}$$

$$q(x,t)=h[T(x,t)-T_\infty] \qquad x\in\Gamma_3 \tag{4}$$

where $\Gamma_1\cup\Gamma_2\cup\Gamma_3=\Gamma$, n is the outward normal to the boundary Γ, h is the heat convective coefficient; $\overline{T}$, $\bar{q}$ and T_∞ are the prescribed temperature, heat flux and surrounding temperature on the boundary, respectively. x_i is the i-th component of the spatial coordinates at point x, λ is thermal conductivity, ρ is density, c is mass specific heat, T is temperature, t represents time, and Q represents the heat source. The repeated subscripts i and j represent the summation through its range which is 2 for 2D and 3 for 3D problems.

3. Element differential method for solving transient nonlinear heat conduction problems

3.1. Shape functions

The heat conduction problem consists of first and second order partial derivatives of temperatures with respect to spatial coordinates. The derivatives are derived by using isoparametric elements. The key mathematical quantities characterizing the isoparametric elements are the shape functions. The shape functions for 1D isoparametric elements can be determined by the Lagrange interpolation formulation [20]:

$$L_I^m(\xi)=\prod_{i=1,i\neq I}^{m}\frac{\xi-\xi_i}{\xi_I-\xi_i} \qquad (I=1\sim m,-1\leqslant\xi\leqslant 1) \tag{5}$$

where m is the number of interpolation points, ξ is the isoparametric coordinate. The shape functions for 2D and 3D problems can be formed based on the 1D shape functions, which can be expressed as follows.

$$N_\alpha(\xi,\eta)=L_I^m(\xi)L_J^n(\eta) \tag{6}$$

for 2D elements, and

$$N_\alpha(\xi,\eta,\zeta)=L_I^m(\xi)L_J^n(\eta)L_K^p(\zeta) \tag{7}$$

for 3D elements.

In Eqs. (5)–(7), the superscripts m, n, and p are the numbers of the interpolation points along ξ, η and ς directions, respectively, and the subscript α is determined by the permutation of the subscripts I, J, and K (for 3D case) [20,24].

3.2. Derivatives of elemental shape functions with respect to global coordinates

Any physical quantity varying over an isoparametric element can be expressed in terms of their nodal values of the element:

$$x_i=N_\alpha x_i^\alpha \tag{8}$$

$$T=N_\alpha T^\alpha \tag{9}$$

where x_i^α and T^α are the values of coordinates and temperature at node α, and the repeated index α represents the summation over all nodes. Based on Eqs. (8) and (9), one can obtain the first and second order derivatives:

$$\frac{\partial T}{\partial x_i}=\frac{\partial N_\alpha}{\partial x_i}T^\alpha \tag{10}$$

$$\frac{\partial^2 T}{\partial x_i \partial x_j} = \frac{\partial^2 N_\alpha}{\partial x_i \partial x_j} T^\alpha \tag{11}$$

where N_α are the explicit functions of intrinsic coordinates ξ_k, thus

$$\frac{\partial N_\alpha}{\partial x_i} = \frac{\partial N_\alpha}{\partial \xi_k}\frac{\partial \xi_k}{\partial x_i} = [J]^{-1}_{ik}\frac{\partial N_\alpha}{\partial \xi_k} \tag{12}$$

$$\frac{\partial^2 N_\alpha}{\partial x_i \partial x_j} = \left[[J]^{-1}_{ik}\frac{\partial^2 N_\alpha}{\partial \xi_k \partial \xi_l} + \frac{\partial [J]^{-1}_{ik}}{\partial \xi_l}\frac{\partial N_\alpha}{\partial \xi_k}\right]\frac{\partial \xi_l}{\partial x_j} \tag{13}$$

where $[J] = [\partial x/\partial \xi]$ is the Jacobian matrix mapping from the global coordinate system x_i to the intrinsic coordinate system ξ_k. For 2D problems, $(x_1, x_2) = (x, y)$ and $(\xi_1, \xi_2) = (\xi, \eta)$. For 3D problems, $(x_1, x_2, x_3) = (x, y, z)$ and $(\xi_1, \xi_2, \xi_3) = (\xi, \eta, \varsigma)$. $\partial \xi_l/\partial x_j$ can be determined by the following matrix relationship:

$$\left[\frac{\partial \xi}{\partial x}\right] = [J]^{-1} = \left[\frac{\partial x}{\partial \xi}\right]^{-1} \tag{14}$$

where

$$\left[\frac{\partial x}{\partial \xi}\right]_{ik} = \frac{\partial x_i}{\partial \xi_k} = \frac{\partial N_\alpha}{\partial \xi_k} x_i^\alpha \tag{15}$$

The analytical expressions of $\frac{\partial N_\alpha}{\partial \xi_k}$ and $\frac{\partial^2 N_\alpha}{\partial \xi_k \partial \xi_l}$ in Eqs. (10) and (11) can be easily obtained by differentiating Eqs. (5)–(7). Then, the key steps are to determine the inverse and derivative matrixes of the Jacobian matrix $[J]$.

For 2D problems, the inverse matrix $[J]^{-1}$ can be easily derived as

$$[J]^{-1} = \frac{1}{|J_2|}\begin{bmatrix} y_\eta & -y_\xi \\ -x_\eta & x_\xi \end{bmatrix} \tag{16}$$

in which, $x_\eta = \partial x/\partial \eta = (\partial N_\alpha/\partial \eta)x^\alpha$, $|J_2| = x_\xi y_\eta - x_\eta y_\xi$.

Also, the term $\partial [J]^{-1}_{ik}/\partial \xi_l$ in Eq. (13) can be derived from Eq. (16) as

$$\frac{\partial [J]^{-1}}{\partial \xi} = \frac{1}{|J_2|^2}\begin{bmatrix} (x_\eta y_{\xi\xi} + x_{\xi\eta} y_\xi - x_{\xi\xi} y_\eta) y_\eta - x_\eta y_\xi y_{\xi\eta}, & (x_{\xi\xi} y_\eta + x_\xi y_{\xi\eta} - x_\eta y_{\xi\xi}) x_\eta - x_\xi x_{\xi\eta} y_\eta \\ (x_{\xi\xi} y_\eta + x_\xi y_{\xi\eta} - x_{\xi\eta} y_\xi) y_\xi - x_\xi y_\eta y_{\xi\xi}, & (x_{\xi\eta} y_\xi + x_\eta y_{\xi\xi} - x_\xi y_{\xi\eta}) x_\xi - x_\eta x_{\xi\xi} y_\xi \end{bmatrix} \tag{17}$$

$$\frac{\partial [J]^{-1}}{\partial \eta} = \frac{1}{|J_2|^2}\begin{bmatrix} (x_{\eta\eta} y_\xi + x_\eta y_{\xi\eta} - x_{\xi\eta} y_\eta) y_\eta - x_\eta y_\xi y_{\eta\eta}, & (x_{\xi\eta} y_\eta + x_\xi y_{\eta\eta} - x_\eta y_{\xi\eta}) x_\eta - x_\xi y_\eta x_{\eta\eta} \\ (x_\xi y_{\eta\eta} + x_{\xi\eta} y_\eta - x_{\eta\eta} y_\xi) y_\xi - x_\xi y_\eta y_{\xi\eta}, & (x_{\eta\eta} y_\xi + x_\eta y_{\xi\eta} - x_\xi y_{\eta\eta}) x_\xi - x_\eta x_{\xi\eta} y_\xi \end{bmatrix} \tag{18}$$

Similar to the 2D problems, the inverse matrix of the Jacobian matrix $[J]$ for 3D problems can be also derived. Then, the first and second order spatial derivatives of shape functions can be calculated and represented by nodal physical quantities.

3.3. Transient state term

The transient term is discretized by using a finite difference scheme, which can be expressed as

$$\rho[T(\boldsymbol{x}, t)]c[T(\boldsymbol{x}, t)]\frac{\partial T(\boldsymbol{x}, t)}{\partial t} = \rho[T(\boldsymbol{x}, t)]c[T(\boldsymbol{x}, t)] \times \frac{T(\boldsymbol{x}, t) - T(\boldsymbol{x}, t - \Delta t)}{\Delta t} \tag{19}$$

where Δt is time step, and $t - \Delta t$ represents the previous time.

The spatial derivatives and the discretized transient term can be substituted into the governing equation and boundary conditions to obtain a system of algebraic equations.

3.4. Assembling system of equations

The computational domain of the problem is first discretized into elements and nodes.

(1). Internal nodes of elements

The governing equation for nodes within an element can be written as:

$$\frac{\partial \lambda_{ij}[T(x,t)]}{\partial x_i}\frac{\partial T(x,t)}{\partial x_j} + \lambda_{ij}[T(x,t)]\frac{\partial^2 T(x,t)}{\partial x_i \partial x_j} + Q(x) = \rho[T(\boldsymbol{x}, t)]c[T(\boldsymbol{x}, t)]\frac{T(\boldsymbol{x}, t) - T(\boldsymbol{x}, t - \Delta t)}{\Delta t} \tag{20}$$

The thermal conductivity is temperature-dependent, so Eq. (20) can be rewritten as:

$$\frac{\partial \lambda_{ij}[T(x,t)]}{\partial T(x,t)}\frac{\partial T(x,t)}{\partial x_i}\frac{\partial T(x,t)}{\partial x_j} + \lambda_{ij}[T(x,t)]\frac{\partial^2 T(x,t)}{\partial x_i \partial x_j} + Q(x) = \rho[T(\boldsymbol{x}, t)]c[T(\boldsymbol{x}, t)]\frac{T(\boldsymbol{x}, t) - T(\boldsymbol{x}, t - \Delta t)}{\Delta t} \tag{21}$$

Substituting Eqs. (10) and (11) into Eq. (21), one can obtain:

$$\left[f\{T[x(\xi), t]\}\frac{\partial N_\beta(\xi)}{\partial x_i}T^\beta\frac{\partial N_\alpha(\xi)}{\partial x_j} + \lambda_{ij}\{T[x(\xi), t]\}\frac{\partial^2 N_\alpha(\xi)}{\partial x_i \partial x_j}\right]T^\alpha + Q[x(\xi)] = \rho\{T[x(\xi), t]\}c\{T[x(\xi), t]\}\frac{T[\boldsymbol{x}(\xi), t] - T[\boldsymbol{x}(\xi), t - \Delta t]}{\Delta t} \tag{22}$$

where ξ is the intrinsic coordinate at the node inside the element under consideration, with$\xi = (\xi, \eta)$ for 2D, and $\xi = (\xi, \eta, \varsigma)$ for 3D problems. f is the derivative of temperature-dependent thermal conductivity with respect to temperature. For each internal node, we can set up an equation by using Eq. (22), which is formulated in terms of the element nodal values of temperature. To solve Eq. (22), the temperatures at the nodes should be known in order to determine the thermophysical properties at the nodes. Therefore, iterative process is required to obtain the final solution.

(2). Element interface nodes

For a node located on the interface shared by a few elements, the relationship between the flux and temperature gradient, Eq. (3), is applied to each surface including the node. In terms of the flux equilibrium condition $\sum_{f=1}^{M} q^f(\xi^I) = 0$, the following equation can be set up by substituting the expressions of shape functions with respect to intrinsic coordinates into Eq. (3).

$$\sum_{f=1}^{M} -\lambda_{ij}\{T^\alpha[x(\xi^I), t]\}\frac{\partial N_\alpha(\xi^I)}{\partial x_j}n_i^f(\xi^I)T^\alpha = 0 \quad \xi^I \in \Gamma_I \tag{23}$$

where M is the number of element surfaces associated with the interface node with intrinsic coordinate ξ^I, the n_i^f is the outward normal to the surface f. Γ_I represents the interface between elements.

It can be seen that the value of temperature at the node α must be known before solving Eq. (23). Since nonlinearity is involved, iterative process is needed.

(3). Outer boundary nodes

For a node located on the outer boundary of the problem, the heat flux equilibrium condition $\sum_{f=1}^{K} q^f(\xi^b) = q(\xi^b)$ is used, where K is the number of element surfaces associated with the boundary node ξ^b, and q is the external heat flux. It follows that:

$$\sum_{f=1}^{K} -\lambda_{ij}\{T^{\alpha}[x(\xi^{l}),t]\}\frac{\partial N_{\alpha}(\xi^{b})}{\partial x_j}n_i^{f}(\xi^{b})T^{\alpha} = q(\xi^{b}) \tag{24}$$

where $q(\xi^b) = \bar{q}$, for $\xi^b \in \Gamma_2$; and $q(\xi^b) = h((\xi^b) - T_\infty)$, for $\xi^b \in \Gamma_3$. Similarly, an iterative process is required, because the value of temperature at the node α is necessary before solving Eq. (24).

Applying the above equations to internal nodes, interface nodes of all elements, and all outer boundary nodes, each of these nodes can generate an equation. Each of the element nodes α corresponds to one position of the global nodes, and the unknowns in the final system of equations are numbered in the global node sequence. For each outer boundary node, either the temperature, the heat flux or convective boundary condition is specified. Thus, the specified temperatures and fluxes are multiplied with corresponding coefficients to form a known vector $\boldsymbol{b}$, which it is moved to the right-hand side of the system of equations. The remaining terms associated with unknown temperatures and unknown fluxes are on the left-hand side of the system of equations. The final system of equations can be formed as

$$\boldsymbol{Ax} = \boldsymbol{b} \tag{25}$$

where $\boldsymbol{x}$ is a vector containing each nodal unknown temperature or unknown flux. By solving Eq. (25) for vector $\boldsymbol{x}$, we can obtain all unknowns of the problem. If the total number of all nodes used to discretize the problem is N, the size of the coefficient matrix $\boldsymbol{A}$ in Eq. (25) is $N \times N$. Since each equation is only related to the nodes of elements associated with the node collocated to this equation, the matrix $\boldsymbol{A}$ is sparse. This feature is in favor of applying a robust sparse matrix equation solver to solve Eq. (25).

The diagonal elements associated with internal nodes of elements in coefficient matrix $\boldsymbol{A}$ and elements associated with internal nodes of elements in vector $\boldsymbol{b}$ are different from those in Refs. [20,24]. If nodes 2, i and N are taken as examples of internal nodes of elements, the elements in matrix $\boldsymbol{A}$ and vector $\boldsymbol{b}$ in this paper are:

$$\mathbf{A} = \begin{bmatrix} a_{11} & a_{12} & \cdots & a_{1N} \\ a_{21} & a_{22} - \frac{\rho(T_0^2)c(T_0^2)}{\Delta t} & \cdots & a_{2N} \\ \vdots & \vdots & \vdots & \vdots \\ a_{i1} & a_{i2} & a_{ii} - \frac{\rho(T_0^i)c(T_0^i)}{\Delta t} & a_{iN} \\ \vdots & \vdots & \vdots & \vdots \\ a_{N1} & a_{N2} & \cdots & a_{NN} - \frac{\rho(T_0^N)c(T_0^N)}{\Delta t} \end{bmatrix} \tag{26}$$

$$\mathbf{b} = \begin{bmatrix} b_1 \\ b_2 - \frac{\rho(T_0^2)c(T_0^2)T_0^2}{\Delta t} \\ \vdots \\ b_i - \frac{\rho(T_0^i)c(T_0^i)T_0^i}{\Delta t} \\ \vdots \\ b_N - \frac{\rho(T_0^N)c(T_0^N)T_0^N}{\Delta t} \end{bmatrix} \tag{27}$$

For each time step, the previous temperature T_0 at each node is known, and the coefficient matrix $\boldsymbol{A}$ contains some assumed temperature values. Thus, an iterative process is required for each time step.

3.5. Iterative methodology for dealing with nonlinearity

For each time step, the solutions of Eq. (25) are based on the values of temperatures at the nodes, which are not all known. Therefore, an iterative process is required, and the methodology is as follows.

The residual vector can be defined as

$$\{R\} = \{b\} - A\{x\} \tag{28}$$

For the i^{th} residual in the vector $\{R\}$, the expression is as follows.

$$R_i = b_i - [A_{i1}\, A_{i2} \quad A_{i3} \quad \dots \quad A_{iN}]\{x\} \tag{29}$$

It can be seen that the residual vector would be zero, if assumed temperatures in the vector $\{x\}$ are exactly the real values. Otherwise, the i^{th} residual for the $(k+1)^{\text{th}}$ iteration can be expanded into Taylor's series as:

$$R_i^{k+1} = R_i^k + \frac{\partial R_i}{\partial x_j}\Delta x_j^k + \frac{1}{2}\frac{\partial^2 R_i}{\partial x_j^2}\{\Delta x_j^2\}^k + \dots \tag{30}$$

Taking only the linear term of Eq. (30), one can obtain:

$$R_i^{k+1} = R_i^k + \frac{\partial R_i}{\partial x_j}\Delta x_j^k \tag{31}$$

Differentiating Eq. (29) with respect to x_j, Eq. (32) can be obtained.

$$\frac{\partial R_i}{\partial x_j} = -\left[\frac{\partial A_{i1}}{\partial x_j}\ \frac{\partial A_{i2}}{\partial x_j}\ \frac{\partial A_{i3}}{\partial x_j}\ \dots\ \frac{\partial A_{iN}}{\partial x_j}\right]\{x\} - [A_{i1}\, A_{i2}\ \ A_{i3}\ \ \dots\ \ A_{iN}]\begin{Bmatrix} \frac{\partial x_1}{\partial x_j} \\ \frac{\partial x_2}{\partial x_j} \\ \vdots \\ \frac{\partial x_N}{\partial x_j} \end{Bmatrix} \tag{32}$$

For the right hand parts of Eq. (32), we only keep the second item. Then, one can obtain Eq. (33).

$$\frac{\partial R_i}{\partial x_j} = -[A_{i1}\, A_{i2} \quad A_{i3} \quad \dots \quad A_{iN}]\begin{Bmatrix} \delta_{1j} \\ \delta_{2j} \\ \vdots \\ \delta_{Nj} \end{Bmatrix} \tag{33}$$

where δ_{mj} is Kronecker delta. If $m = j$, it equals 1. Otherwise, it equals 0. Therefore, there is only one item 1 remained for $\{\delta\}$ vector, under the condition that i equals j. Then, we can obtain Eq. (34).

$$\frac{\partial R_i}{\partial x_j} = -A_{ij} \tag{34}$$

Therefore, Eq. (35) could be obtained by expanding Eq. (29) into the vector form based on Eq. (34).

$$\{R\}^{k+1} = \{R\}^k - A^k\{\Delta x\}^k \tag{35}$$

Assuming $\{R\}^{k+1}$ equals zero, one can obtain Eq. (36).

$$\{\Delta x\}^k = [A^k]^{-1}\{R\}^k \tag{36}$$

Then the $\boldsymbol{x}$ vector can be updated by Eq. (37).

$$\{x\}^{k+1} = \{x\}^k + w\{\Delta x\}^k \tag{37}$$

where w is a relaxation factor.

The iteration is terminated until the residual error is within a certain limit. Otherwise, the iterative process continues with updated assumed values.

4. Results and discussions

4.1. Example 1

In the first example, a square of $10 \times 10\ \text{cm}^2$ is considered, and the initial temperatures are 100 °C. The heat source is constant,

and the value is 1000 W/m^3. The temperature-dependent thermal conductivity is

$$\lambda(T) = 100 + 0.1T \tag{38}$$

The density and specific heat are 7000 kg/m^3 and 465 J/(kg °C), respectively.

Temperatures on the left boundary are kept as 100 °C, and the right boundary is suddenly imposed 110 °C. Other boundaries are insulated. The time is 60 s, and the time step is 0.5 s.

The meshes by using the EDM are shown in Fig. 1, which have been validated by grid independence test; there are 441 nodes and 100 9-node elements. As expected, the temperature field by using the EDM is with one-dimensional distribution. For quantitatively evaluating the results by using the EDM, the finite element method is employed to solve the transient nonlinear heat conduction problem, and Table 1 lists the transient temperatures along the x-direction. It can be seen that the results of the EDM are in very good agreement with those of the FEM, and the maximal relative error is only 0.61%, which indicates that the EDM is with very high accuracy for solving a 2D transient nonlinear heat conduction problem with heat source in a regular 2D geometry.

4.2. Example 2

In the second example, an irregular 2D geometry is considered, and the EDM model is shown in Fig. 2, which has been checked by grid independence test. There are 3264 nodes and 768 elements.

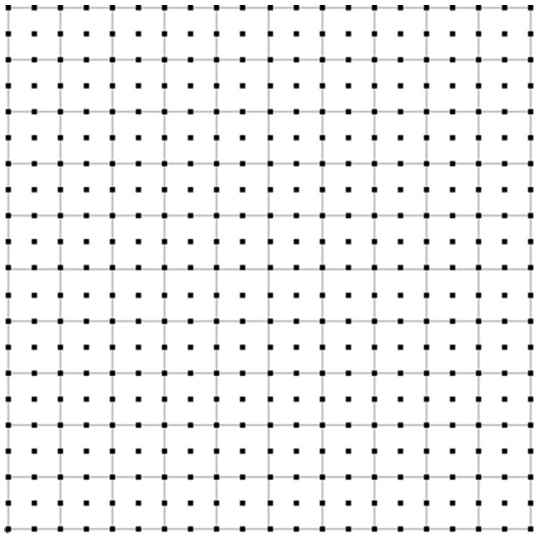

Fig. 1. EDM model for the 2D square.

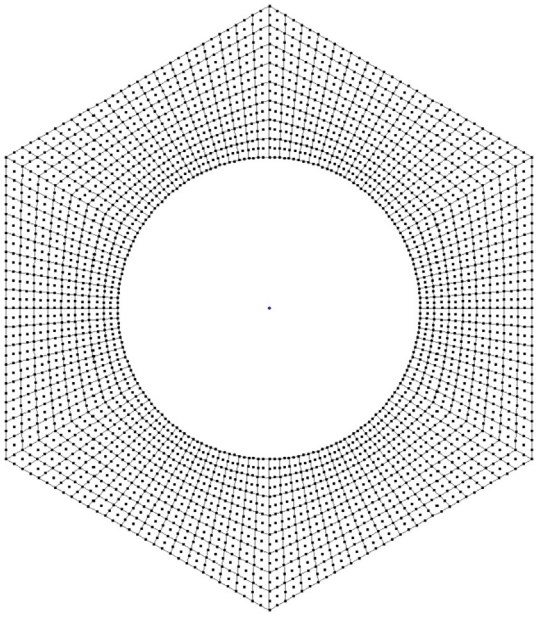

Fig. 2. EDM model for the irregular 2D geometry.

The side length of the hexagon is 0.2 m, and the radius of the circular is 0.1 m.

In the transient nonlinear heat conduction problem, the initial temperatures are 1200 °C, and the heat source is varying with both the x- and y-coordinates:

$$Q(x) = 200 + 500\sqrt{x^2 + y^2} \tag{39}$$

The temperature-dependent thermal conductivity is:

$$\lambda(T) = 40 + 0.01T + 10^{-5}T^2 \tag{40}$$

the density and specific heat are 7800 kg/m^3 and 465 J/(kg °C), respectively.

The outer boundary is insulated, and the inner boundary is imposed on constant heat flux, and the value is −50,000 W/m^2. The time is 10 s, and the time step is 0.05 s. Fig. 3 shows the transient temperature field. It can be seen that the entire structure is gradually cooled, and the temperature decreases from the inner boundary to the outer boundary. This is because constant cooling heat flux is imposed on the inner boundary, and the outer boundary is insulated. For comparison, the finite element method is adopted to solve the problem, and there are also 768 4-node elements. The transient temperature field is exactly the same as those in Fig. 3, and the temperature relative error is all less than 0.1%, which reveals the high accuracy of the present EDM for solving a

Table 1
Transient temperatures by using the EDM and FEM in a regular 2D geometry.

x, m	Temperature, °C					
	20 s		40 s		60 s	
	EDM	FEM	EDM	FEM	EDM	FEM
0.01	100.12	100.16	100.49	100.44	100.74	100.67
0.02	100.29	100.35	101.03	100.92	101.50	101.37
0.03	100.57	100.61	101.66	101.48	102.32	102.12
0.04	101.03	100.99	102.42	102.17	103.20	102.96
0.05	101.73	101.55	103.33	103.02	104.15	103.89
0.06	102.76	102.38	104.40	104.05	105.20	104.94
0.07	104.14	103.56	105.64	105.29	106.32	106.09
0.08	105.86	105.22	107.01	106.73	107.50	107.33
0.09	107.85	107.40	108.48	108.32	108.74	108.65

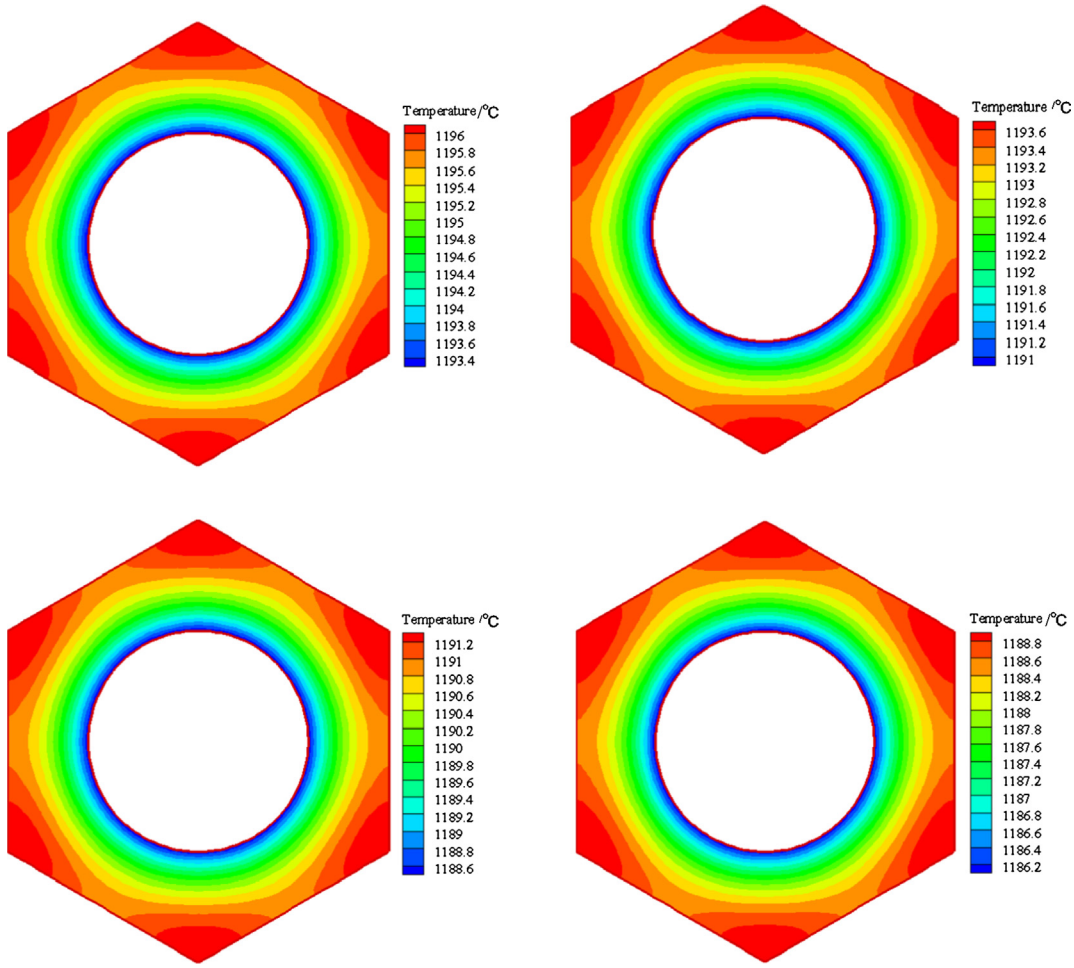

Fig. 3. Transient temperature field in the irregular 2D geometry: (a) 4 s; (b) 6 s; (c) 8 s; (d) 10 s.

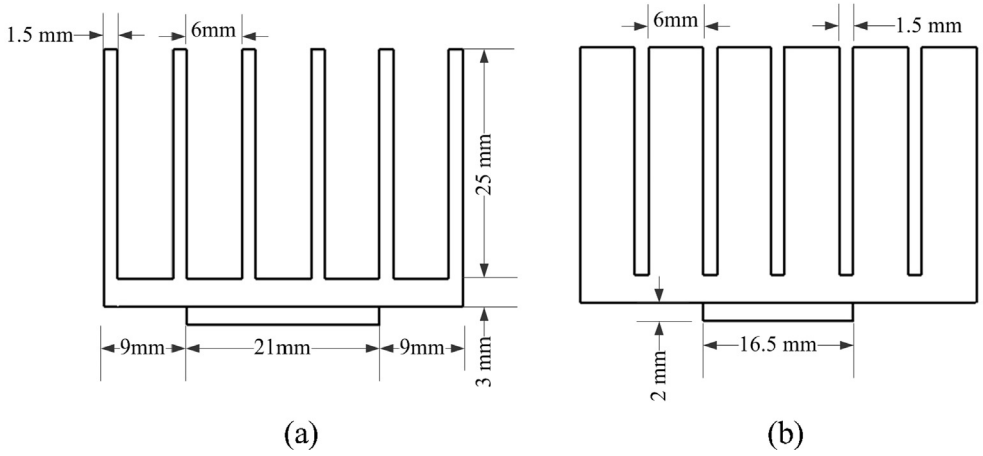

Fig. 4. Geometrical dimensions of the heat radiator: (a) front view; (b) left view.

transient nonlinear heat conduction problem in an irregular 2D geometry.

4.3. Example 3

Finally, a complex 3D geometry is considered. A heat radiator with 6 × 6 cooling fins is taken as the example, and the geometrical dimensions are the same as those in Ref. [25], which are shown in Fig. 4.

There is a heat source, and the value is 600 W/ m^3. The density and the specific heat are 8900 kg/m^3 and 390 J/(kg °C), respectively. The temperature-dependent thermal conductivity is (340 + 0.2 T) W/(m °C). The temperature on the bottom boundary is 200 °C, and other boundaries of the radiator are cooled by convective heat transfer. The convective heat transfer coefficient h and the ambient temperature T_f are 5 W/(m^2 °C) and 20 °C, respectively. The initial temperatures are 25 °C, and the time step being 0.2 s. Fig. 5 shows the EDM model, and there are 178,995 nodes and

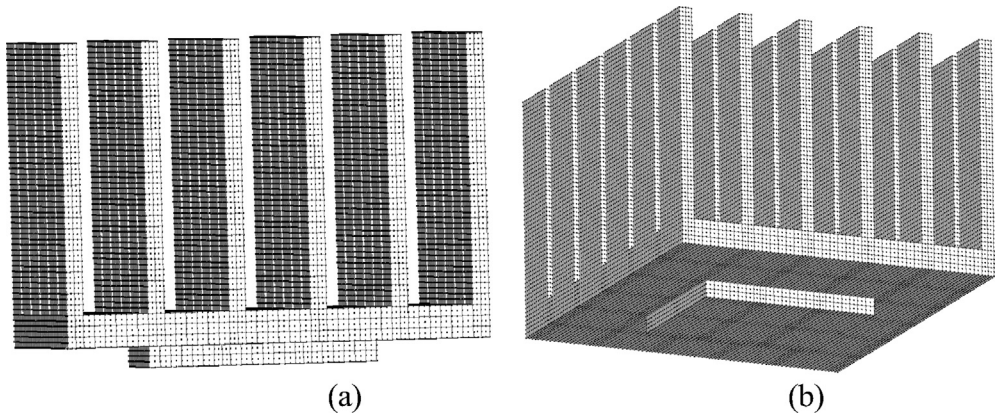

Fig. 5. EDM model for the 3D heat radiator: (a) nearly front view; (b) nearly left view.

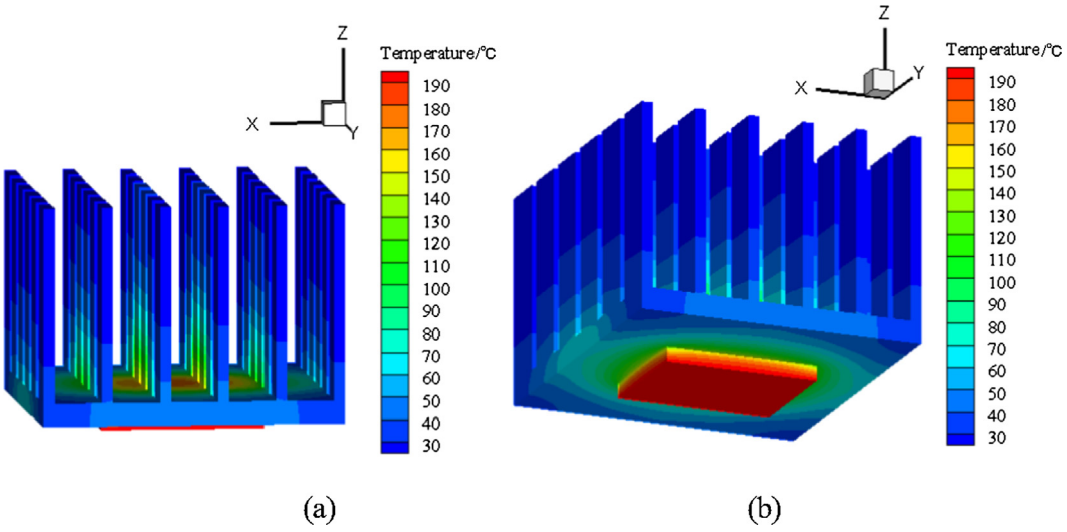

Fig. 6. Transient temperature field in the 3D heat radiator, when the time is 0.6 s: (a) nearly front view; (b) nearly left view.

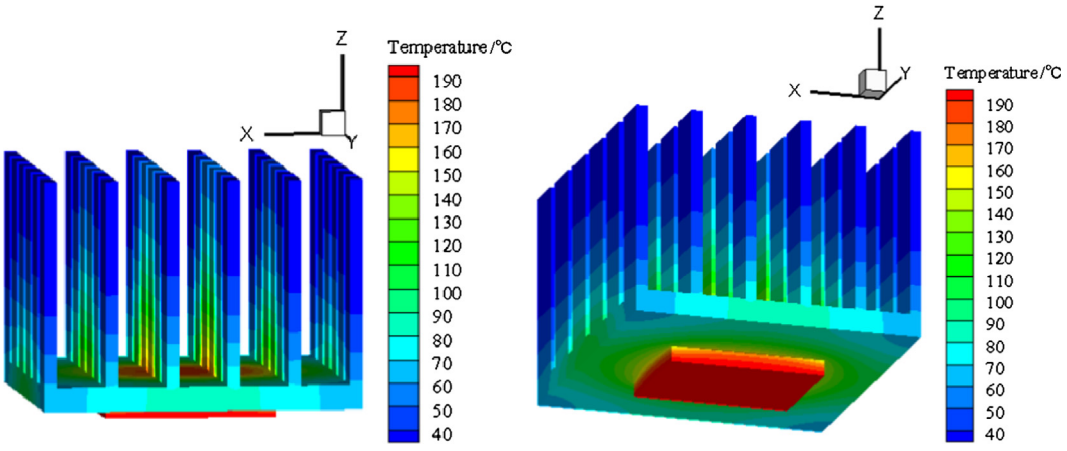

Fig. 7. Transient temperature field in the 3D heat radiator, when the time is 1.4 s: (a) nearly front view; (b) nearly left view.

17,388 elements. Figs. 6–8 show the transient temperature field in the 3D heat radiator, when the time is 0.6 s, 1.4 s and 2.2 s, respectively.

It can be seen that the heat conducts very quickly from the bottom to other positions. This is because the temperature-dependent thermal conductivity is with a large value. The temperature is increasing although the other surfaces are cooled by convection, and it is because the cooling could not overwhelm the heating effect. The highest temperature is located at the bottom surface. The heat conducts from the bottom surface to the upper surface, which spreads from the upper surface center to the sides and the fins.

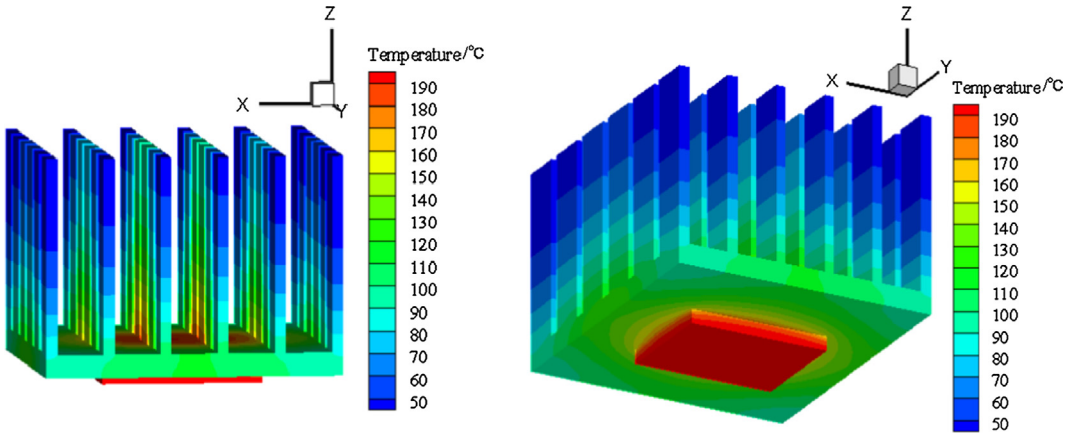

Fig. 8. Transient temperature field in the 3D heat radiator, when the time is 2.2 s: (a) nearly front view; (b) nearly left view.

Table 2
Temperatures by using the EDM and the FEM in the 3D heat radiator at 2.2 s.

y, mm	Temperature, °C		Relative error, %
	EDM	FEM	
7.5	128.03	127.47	0.44
15.0	176.86	176.22	0.36
22.5	190.06	189.55	0.27
30.0	167.85	167.21	0.38
37.5	120.97	120.38	0.49

Table 3
Computational time by using the EDM and the FEM in ANSYS.

	Computational time, s	
	EDM	FEM
Example 1	79.70	11.52
Example 2	849.88	34.42
Example 3	14320.32	37.51

For quantitatively evaluating the accuracy of the EDM, the FEM is also employed, and there are 17,388 elements. Transient temperatures at some typical points (x = 19.5 mm, z = 3 mm) are selected and compared, which are listed in Table 2. It can be seen that the results of the EDM agree well with those by using the FEM, and the maximal relative error is less than 0.5%, which implies the high accuracy of the present EDM for solving a transient nonlinear heat conduction problem in a 3D complex geometry.

4.4. Computational time

The computational time of the present EDM for solving the above transient nonlinear heat conduction problems with heat sources is also compared with that by using the FEM in ANSYS, which is shown in Table 3. The computer has an Intel Core 2 Duo 2.93 GHz CPU, 4.0 GB of memory. The grids for the EDM are the same as those in the above three examples, and the grids for the FEM are the sparsest which have been checked by grid independence. It means that the computational time by using the FEM is the least in Table 3. It can be seen that the present EDM is less efficient than the FEM for solving transient nonlinear heat conduction problems with heat sources, which is one disadvantage of the present EDM. It is mainly caused by slow process of forming system of equations in the EDM. Meanwhile, the iterative process caused by the nonlinearity also slows down the efficiency. Further work is needed to improve the efficiency of the present EDM. Numerical tests also show that the grid resolution needs to be generally higher by using the present EDM for solving transient nonlinear heat conduction problems with heat sources. This is another reason why the present EDM is less efficient than the FEM.

5. Conclusions

The element differential method has the advantage that no any mathematical principles or integrations are required, and it is very easy to code. In the present work, the EDM is extended to solve multi-dimensional transient nonlinear heat conduction problems for the first time. The transient term is discretized by using a finite difference scheme, and an iterative technique is developed to deal with the nonlinearity. The 2D and 3D examples show that the present EDM is effective and with high accuracy for solving a multi-dimensional transient nonlinear heat conduction problem with a heat source. The present EDM and the codes would be very convenient to be applied in inverse analysis by using the complex variable differentiation method for sensitivity analysis. One disadvantage of the present EDM is that it is less efficient than the FEM in commercial software, for solving transient nonlinear heat conduction problems with heat sources.

Conflict of interest

None declared.

Acknowledgment

Financial support of this work by the National Nature Science Foundation of China (51576026, 11672061), the China Postdoctoral Science Foundation (2016M601305), and the Fundamental Research Funds for the Central Universities (DUT17LK04) is gratefully acknowledged.

References

[1] A. Riccio, F. Raimondo, A. Sellitto, V. Carandente, R. Scigliano, Optimum design of ablative thermal protection systems for atmospheric entry vehicles, Appl. Therm. Eng. 119 (2017) 541–552.
[2] J. Ma, Y.S. Sun, B.W. Li, Simulation of combined conductive, convective and radiative heat transfer in moving irregular porous fins by spectral element method, Int. J. Therm. Sci. 118 (2017) 475–487.
[3] P.A. Isaza, A.O. Brien, W.D. Warnica, M. Bussmann, Assessing axial heat conduction in moving bed heat exchangers, Int. J. Therm. Sci. 120 (2017) 303–313.
[4] M. Cui, J. Mei, B.W. Zhang, B.B. Xu, L. Zhou, Y.W. Zhang, Inverse identification of boundary conditions in a scramjet combustor with a regenerative cooling system, Appl. Therm. Eng. 134 (2018) 555–563.

[5] Z.X. Tong, M.J. Li, J.J. Yan, W.Q. Tao, Optimizing thermal conductivity distribution for heat conduction problems with different optimization objectives, Int. J. Heat Mass Transf. 119 (2018) 343–354.
[6] T.A. Annafi, A.A. Gyeabour, E.H.K. Akaho, M. Annor-Nyarko, C.R. Quaye, Finite difference analysis of the transient temperature profile within GHARR-1 fuel element, Ann. Nucl. Energy 68 (2014) 204–208.
[7] M. Cui, Y. Zhao, B.B. Xu, S.D. Wang, X.W. Gao, Inverse analysis for simultaneously estimating multi-parameters of temperature-dependent thermal conductivities of an Inconel in a reusable metallic thermal protection system, Appl. Therm. Eng. 125 (2017) 480–488.
[8] W. Li, B. Yu, X.R. Wang, P. Wang, S.Y. Sun, A finite volume method for cylindrical heat conduction problems based on local analytical solution, Int. J. Heat Mass Transf. 55 (2012) 5570–5582.
[9] S. Han, Finite volume solution of two-step hyperbolic conduction in casting sand, Int. J. Heat Mass Transf. 93 (2016) 1116–1123.
[10] F. Clarac, F. Goussard, L. Teresi, V. Buffrenil, V. Sansalone, Do the ornamented osteoderms influence the heat conduction through the skin? A finite element analysis in Crocody lomorpha, J. Therm. Bio. 69 (2017) 39–53.
[11] A. Cebula, J. Taler, P. Ocłoń, Heat flux and temperature determination in a cylindrical element with the use of Finite Volume Finite Element Method, Int. J. Thermal Sci. 127 (2018) 142–157.
[12] J. Sladek, V. Sladek, Ch. Zhang, Transient heat conduction analysis in functionally graded materials by the meshless local boundary integral equation method, Comput. Mater. Sci. 28 (2003) 494–504.
[13] G.R. Joldes, H. Chowdhury, A. Wittek, K. Miller, A new method for essential boundary conditions imposition in explicit meshless methods, Eng. Anal. Boundary Elem. 80 (2017) 94–104.
[14] L.C. Wrobel, C.A. Brebbia, Boundary Element Methods in Heat Transfer, Computational Mechanics Publications, Southampton Boston, 1992.
[15] B. Yu, C. Xu, W.A. Yao, Z. Meng, Estimation of boundary condition on the furnace inner wall based on precise integration BEM without iteration, Int. J. Heat Mass Transf. 122 (2018) 823–845.
[16] M. Cui, H.F. Peng, B.B. Xu, X.W. Gao, Y.W. Zhang, A new radial integration polygonal boundary element method for solving heat conduction problems, Int. J. Heat Mass Transf. 123 (2018) 252–260.
[17] J. Ling, D.S. Yang, B.W. Zhai, Z.H. Zhao, T.Y. Chen, Z.X. Xu, H. Gong, Solving the single-domain transient heat conduction with heat source problem by virtual boundary meshfree Galerkin method, Int. J. Heat Mass Transf. 115 (2017) 361–367.
[18] Y.C. Hua, T. Zhao, Z.Y. Guo, Optimization of the one-dimensional transient heat conduction problems using extended entransy analyses, Int. J. Heat Mass Transf. 116 (2018) 166–172.
[19] W. Choi, R. Ooka, M. Shukuya, Exergy analysis for unsteady-state heat conduction, Int. J. Heat Mass Transf. 116 (2018) 1124–1142.
[20] X.W. Gao, S.Z. Huang, M. Cui, B. Ruan, Q.H. Zhu, K. Yang, J. Lv, H.F. Peng, Element differential method for solving general heat conduction problems, Int. J. Heat Mass Transf. 115 (2017) 882–894.
[21] M. Cui, X.W. Gao, J.B. Zhang, A new approach for the estimation of temperature-dependent thermal properties by solving transient inverse heat conduction problems, Int. J. Therm. Sci. 58 (2012) 113–119.
[22] M. Cui, Y. Zhao, B.B. Xu, X.W. Gao, A new approach for determining damping factors in Levenberg-Marquardt algorithm for solving an inverse heat conduction problem, Int. J. Heat Mass Transf. 107 (2017) 747–754.
[23] M. Cui, L. Zhou, J. Mei, B.W. Zhang, Estimation of slab surface radiative emissivities by solving an inverse coupled conduction, convection, and radiation problem, Numer. Heat Transfer, Part A: Appl. 72 (10) (2017) 765–779.
[24] X.W. Gao, Z.Y. Li, K. Yang, J. Lv, H.F. Peng, M. Cui, B. Ruan, Q.H. Zhu, Element differential method and its application in thermal-mechanical problems, Int. J. Numer. Meth. Eng. 113 (2018) 82–108.
[25] X.W. Gao, H.Y. Liu, B.B. Xu, M. Cui, J. Lv, Element differential method with the simplest quadrilateral and hexahedron quadratic elements for solving heat conduction problems, Numer. Heat Transfer, Part B: Fund. (in press). https://doi.org/10.1080/10407790.2018.1461491.